

Uncertainty-aware Pseudo-label Selection for Positive-Unlabeled Learning

Emilio Dorigatti^{1,2,3}, Jann Goschenhofer^{1,3,4}, Benjamin Schubert^{2,5}, Mina Rezaei¹
and Bernd Bischl^{1,3,4}

¹Department of Statistics, Ludwig-Maximilians-Universität München, München 80539, Germany

²Institute of Computational Biology, Helmholtz Zentrum München—German Research Center for Environmental Health, Neuherberg 85764, Germany

³Munich Center for Machine Learning, München, Germany

⁴Fraunhofer Institute for Integrated Circuits IIS, Erlangen 91058, Germany

⁵Department of Mathematics, Technical University of Munich, Garching bei München 85748, Germany

March 12, 2024

Abstract: Positive-unlabeled learning (PUL) aims at learning a binary classifier from only positive and unlabeled training data. Even though real-world applications often involve imbalanced datasets where the majority of examples belong to one class, most contemporary approaches to PUL do not investigate performance in this setting, thus severely limiting their applicability in practice. In this work, we thus propose to tackle the issues of imbalanced datasets and model calibration in a PUL setting through an uncertainty-aware pseudo-labeling procedure (*PUUPL*): by boosting the signal from the minority class, pseudo-labeling expands the labeled dataset with new samples from the unlabeled set, while explicit uncertainty quantification prevents the emergence of harmful confirmation bias leading to increased predictive performance. Within a series of experiments, PUUPL yields substantial performance gains in highly imbalanced settings while also showing strong performance in balanced PU scenarios across recent baselines. We furthermore provide ablations and sensitivity analyses to shed light on PUUPL’s several ingredients. Finally, a real-world application with an imbalanced dataset confirms the advantage of our approach.

Keywords: Uncertainty Quantification, Self-supervised Learning, Positive Unlabeled Learning, Imbalanced Data

1 Introduction

Many real-world applications involve positive-unlabeled (PU) datasets Armenian and Lilienfeld [1974], Gligorijević et al. [2021], Purcell et al. [2019] in which only a few samples are labeled positive while the majority is unlabeled. PU learning (PUL) aims to learn a binary classifier in this challenging setting without any labeled negative examples, thus reducing the need for manual annotation and enabling entirely new applications where negative examples are costly or impossible to obtain [Kiryo et al., 2017]. Learning from PU data can reduce development costs in many deep learning applications that otherwise require costly annotations from experts or expensive experimental procedures such as medical image diagnosis Armenian and Lilienfeld [1974] and protein function prediction Gligorijević et al. [2021]. PUL can even enable applications

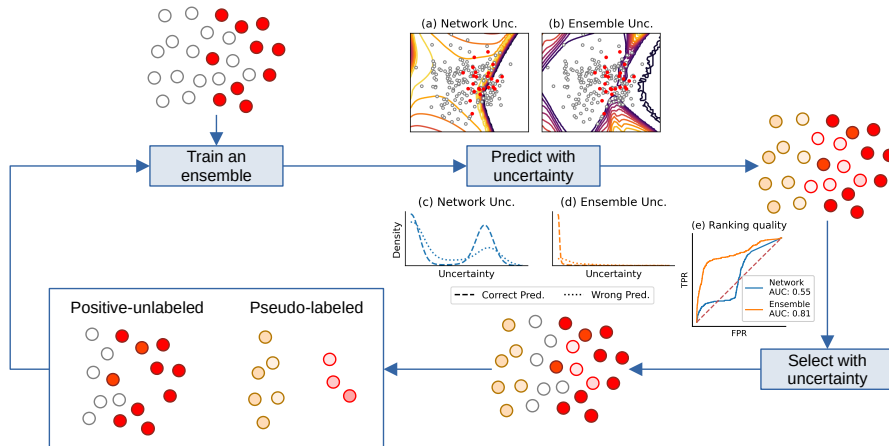


Figure 1: *PUUPL* is a pseudo-labeling framework for PU learning that uses the epistemic uncertainty of an ensemble to select confident examples to pseudo-label. The ensemble can be trained with any PU loss for PU data while minimizing the cross-entropy loss on the previously assigned pseudo-labels. In a toy example, a single network is not very confident on most of the unlabeled data (a), resulting in many high-confidence incorrect predictions and many low-confidence correct ones (c). The epistemic uncertainty of an ensemble is, on the other hand, very low on most of the unlabeled data (b), resulting in most correct predictions having low uncertainty and most incorrect predictions having high uncertainty (d). Thus, the estimated uncertainty by ensemble can be used more reliably to rank predictions and select correct ones (e). Re-training the model with an increased number of labeled samples will result in a slightly more accurate model, than can be used to predict new pseudo-labels, which will further improve the model’s performance, etc.

in settings where the measurement technology itself can not detect negative examples Purcell et al. [2019].

Many PUL applications share another intrinsic difficulty: class imbalance. Imbalanced settings arise when most samples in a dataset belong to the same class, and frequently the most interesting class happens to be the minority. In PUL, class imbalance refers specifically to a low class prior $\pi := p(y = 1)$ implying that the majority of the unlabeled samples are negatives. While this problem can be tackled in traditional (semi-)supervised learning by re-weighting the loss to increase the penalty of mis-classification of the minority class, a similar approach was introduced in PUL with some additional care in handling the unlabeled data points [Su et al., 2021]. However, the issue remains in general under-studied in the literature and recent developments such as Self-PU [Chen et al., 2020b] are solely targeted at balanced scenarios.

Motivated by this, we propose to tackle imbalancedness in PUL via pseudo-labeling [Lee, 2013], an iterative procedure that augments the labeled dataset with new samples from the unlabeled set, thus boosting the weak signal from the minority class. To prevent the emergence of harmful confirmation bias in this procedure, we propose to assign pseudo-labels based on likelihood-free uncertainty quantification via model ensembling [Lakshminarayanan et al., 2017]. By using soft targets we avoid artificially inflating the confidence of pseudo-labels and preserve the calibration signal for the ensemble in later training iterations, thus eventually obtaining a predictor that is both calibrated and well-performing. Another advantage of pseudo-labeling is that it allows the model to harness the power of self-training without requiring modality-specific augmentations such as MixUp [Zhang et al., 2018] that restrict most contemporary PUL methods [Chen et al., 2020a, Hammoudeh and Lowd, 2020, Acharya et al., 2022, Chen et al.,

2020b, Zhao et al., 2022] to image data only.

To summarize, our contributions are:

1. We introduce *PUUPL* (Positive UnlabeledUncertainty aware Pseudo-Labeling), a novel framework that successfully overcomes the issue of imbalanced data distribution in PUL in a data-modality-agnostic framework while retaining competitive performance on balanced datasets.
2. We evaluate our methods on a wide range of benchmarks and PU datasets, achieving state-of-the-art results in self-training for PUL both with and without knowing the positive class prior π . Our results show that PUUPL is applicable to different data modalities such as images and text, can use any risk estimator for PUL and improve thereupon, and is robust to prior misspecification and class imbalance.
3. We apply PUUPL to a real-world healthcare dataset, confirming the advantage of PUUPL compared to other PUL methods as well as previous domain-specific state-of-the-art approaches.

These results demonstrate that our framework is highly reliable, extensible, and applicable in a variety of real-world scenarios.

2 Related work

PUL was introduced as a variant of binary classification Liu et al. [2003] and is related to one-class learning Ruff et al. [2018], Li et al. [2010], multi-positive learning Xu et al. [2017], multi-task learning Kaji et al. [2018], and semi-supervised learning Chapelle et al. [2009]. Current existing methods for PUL can be divided into three branches: two-step techniques, class prior incorporation, and biased PUL Bekker and Davis [2020]. In this work, we apply pseudo-labeling with biased PUL – also coined as re-weighting methods – and refer to Bekker et al. Bekker and Davis [2020] for a comprehensive overview of the field. In this context, Du Plessis et al. Du Plessis et al. [2014] introduced the unbiased risk estimator uPU. Kiryo et al. Kiryo et al. [2017] showed that this loss function is prone to overfitting in deep learning contexts, as it lacks a lower bound, and proposed the non-negative risk estimator nnPU Kiryo et al. [2017] as a remedy. Follow-up work on loss functions for PUL has focused on robustness w.r.t. biases in the sampling process Kato et al. [2019], Hsieh et al. [2019], Luo et al. [2021] and handling of imbalanced datasets Su et al. [2021]. Further research in PUL focuses on estimating the class prior directly during training Chen et al. [2020a], Garg et al. [2021], Hu et al. [2021] or exploiting its knowledge to further improve the training process Chen et al. [2020b], Acharya et al. [2022], Zhao et al. [2022], Hammoudeh and Lowd [2020].

Pseudo-labeling [Lee, 2013] is a popular approach for semi-supervised learning when several unlabeled examples are available. In pseudo-labeling, the model leverages its own predictions on unlabeled data as training targets to enable iterative semi-supervised model training. However, erroneously selected pseudo-labels can amplify errors during training, potentially leading to model degradation over time. This *confirmation bias* is grounded in poor model calibration which distorts the signal for the pseudo label selection Van Engelen and Hoos [2020], and is exacerbated in a deep learning setting as deep neural networks are prone to over-confident predictions unless trained appropriately Gawlikowski et al. [2021]. A variety of approaches were proposed for semi-supervised classification settings to mitigate this problem [Isken et al., 2019, Shi et al., 2018, Arazo et al., 2020, Tanaka et al., 2018, Rizve et al., 2021, Beluch et al., 2018]:

the commonality of these works is the explicit consideration of model uncertainty to improve pseudo-label selection, which motivates its application in the context of PUL.

A first attempt to combine pseudo-labeling with PUL was made with Self-PU Chen et al. [2020b], where self-paced learning, a confidence-weighting scheme based on the model predictions, and a teacher-student distillation approach are combined. With *PUUPL*, we propose an alternative pseudo-labeling strategy for PUL that performs better in a simpler and more principled way using implicitly well-calibrated models to improve the pseudo-label selection. Moreover, uncertainty awareness allows *PUUPL* to work well in unbalanced data environments where Self-PU breaks down. To the best of our knowledge, we are the first to introduce an uncertainty-aware pseudo-labeling paradigm to PUL. Although our method shares the same motivation as that from Rizve et al. [2021] for semi-supervised classification with both positive and negative training samples, we differ in several important aspects dictated by the PUL setting: (1) we specifically target PU data with a PU loss, (2) we quantify uncertainty with an ensemble instead of Monte Carlo dropout, (3) we use epistemic uncertainty instead of the predicted class probabilities for the selection, (4) we do not use temperature scaling and (5) use soft labels.

3 Method

PUUPL (Algorithm 1) separates the training set X^{tr} into the sets P , U , and L , which contain the initial positives, the currently unlabeled, and the pseudo-labeled samples, respectively. The set L is initially empty. At each pseudo-labeling iteration, we first train our model using all samples in P , U , and L until some convergence condition is met (Section 3.2). Then, model predictions over the samples in U are ranked w.r.t. their predictive uncertainty (Section 3.3), and samples with the most confident score are assigned the predicted label and moved into the set L (Section 3.4). Similarly, model predictions are derived for the samples in L , and the most uncertain samples are moved back to the unlabeled set U (Section 3.5). Next, the model is re-initialized to the same initial weights, and the next pseudo-labeling iteration starts.

3.1 Notation

Consider input samples X with label y and superscripts $.^{tr}$, $.^{va}$ and $.^{te}$ for training, validation, and test data, respectively. The initial training labels y^{tr} are set to one for all samples in P and zero for all others in U . We group the indices of original positives, unlabeled, and pseudo-labeled samples in X^{tr} into the sets P , U , and L , respectively, where $y_i = 1$ for $i \in P$, $y_i = 0$ for $i \in U$, and y_i is the assigned pseudo-label for $i \in L$. Our proposed model is an ensemble of K deep neural networks whose random initial weights are collectively denoted as θ^0 . The predictions of the k -th network for sample i are indicated with $\hat{p}_{ik} = \sigma(\hat{f}_{ik})$, with $\sigma(\cdot)$ as the logistic function and \hat{f}_{ik} as the predicted logits. The logits and predictions for a sample averaged across the networks in the ensemble are denoted by \hat{f}_i and \hat{p}_i , respectively. We subscript data and predictions with i to index individual samples, and use an index set in the subscript to index all samples in the set (e.g., $X_U^{tr} = \{x_i^{tr} | i \in U\}$ denotes the features of all unlabeled samples). We denote the total, epistemic, and aleatoric uncertainty of sample i as \hat{u}_i^t , \hat{u}_i^e , and \hat{u}_i^a , respectively.

3.2 Loss function

We train our proposed model with a loss function \mathcal{L} that is a convex combination of a loss \mathcal{L}_{PU} for the samples in the positive and unlabeled set ($P \cup U$) and a loss \mathcal{L}_L for the samples in the pseudo-labeled set (L):

$$\mathcal{L} = \lambda \cdot \mathcal{L}_L + (1 - \lambda) \cdot \mathcal{L}_{PU} \tag{1}$$

Algorithm 1 The PUUPL Training Procedure

Hyperparameters:

- Loss mixing coefficient λ
- Number K of networks in the ensemble
- Maximum number T of pseudo-labels to assign at each round
- Maximum uncertainty threshold t_l to assign pseudo-labels
- Minimum uncertainty threshold t_u to remove pseudo-labels

Input: Train and validation $X^{tr}, y^{tr}, X^{va}, y^{va}$

- 1: $P \leftarrow$ indices of positive samples in X^{tr}
 - 2: $U \leftarrow$ indices of unlabeled samples in X^{tr}
 - 3: $L \leftarrow \emptyset$
 - 4: $\theta^0 \leftarrow$ Random weight initialization
 - 5: **while** not converged **do**
 - 6: Initialize model weights to θ^0
 - 7: Train an ensemble of K networks on X^{tr}, y^{tr}
 - 8: Update θ^* if performance on X^{va}, y^{va} improved
 - 9: $\hat{f} \leftarrow$ ensemble predictions for X^{tr}
 - 10: Compute epistemic uncertainty via Eq. 7
 - 11: $L^{\text{new}} \leftarrow$ Examples to pseudo-label via Eq. 8
 - 12: $U^{\text{new}} \leftarrow$ Examples to pseudo-unlabel
 - 13: $L \leftarrow L \cup L_b^{\text{new}} \setminus U^{\text{new}}$
 - 14: $U \leftarrow U \setminus L_b^{\text{new}} \cup U^{\text{new}}$
 - 15: $y_{L^{\text{new}}} \leftarrow \hat{p}_{L^{\text{new}}}$
 - 16: $y_{U^{\text{new}}} \leftarrow 0$
 - 17: **end while**
-

with $\lambda \in (0, 1)$. The loss \mathcal{L}_L is the binary cross-entropy computed w.r.t. the assigned pseudo-labels. Our method is agnostic to the specific PU loss \mathcal{L}_{PU} used, allowing PUUPL to be easily adapted to provide further performance increase in other scenarios for which a different PU loss might be more appropriate, e.g., when a set of biased negative samples is available Hsieh et al. [2019], when coping with a selection bias in the positive examples Kato et al. [2019] or an imbalanced class distribution Su et al. [2021] (see experiments). For the standard setting of imbalanced PUL, we use the imbnnPU loss [Su et al., 2021]:

$$\mathcal{L}_{PU} = \pi' \ell(P, 1) + \max \left\{ 0, \frac{1 - \pi'}{1 - \pi} \ell(U, -1) - \frac{(1 - \pi')\pi}{1 - \pi} \ell(P, -1) \right\} \quad (2)$$

where $\pi = p(y = 1)$ is the prior probability that a sample is positive, π' the desired oversampled probability that we fix to 1/2, and $\ell(S, y)$ the eWe do not run bibtex in the auto-TeXing procedure. If you use bibtex, you must compile the .bbl file on your computer then include that in your uploaded expected sigmoid loss of samples in the set S with label y :

$$\ell(S, y) = \frac{1}{|S|} \sum_{i \in S} \frac{1}{1 + \exp(y \cdot \hat{p}_i)} \quad (3)$$

Similarly, we use the non-negative correction $nnPU$ of the PU loss Kiryo et al. [2017] for the standard, balanced PU setting:

$$\mathcal{L}_{PU} = \pi \cdot \ell(P, 1) + \max \{0, \ell(U, -1) - \pi \cdot \ell(P, -1)\} \quad (4)$$

where $\pi := p(y = 1)$ is the prior probability that a sample is positive and $\ell(S, y)$ follows equation 3.

While π can be estimated from PU data Christoffel et al. [2016], in our experimental results we treat π as a hyperparameter and optimize it without requiring negatively labeled samples via a PU validation set Menon et al. [2015].

3.3 Model uncertainty

We utilize a deep ensemble with K networks with the same architecture, each trained on the full training dataset Lakshminarayanan et al. [2017], to quantify the predictive uncertainty. Given the predictions $\hat{p}_{i1}, \dots, \hat{p}_{iK}$ for a sample x_i , we associate three types of uncertainties to x_i 's predictions Hüllermeier and Waegeman [2021]: the aleatoric uncertainty as the mean of the entropy of the predictions (Eq. 5), the total uncertainty as the entropy of the mean prediction (Eq. 6), and the epistemic uncertainty formulated as the difference between the two (Eq. 7).

$$\hat{u}_i^a = -\frac{1}{K} \sum_{k=1}^K [\hat{p}_{ik} \log \hat{p}_{ik} + (1 - \hat{p}_{ik}) \log(1 - \hat{p}_{ik})] \quad (5)$$

$$\hat{u}_i^t = -\hat{p}_i \log \hat{p}_i - (1 - \hat{p}_i) \log(1 - \hat{p}_i) \quad (6)$$

$$\hat{u}_i^e = \hat{u}_i^t - \hat{u}_i^a \quad (7)$$

where $\hat{p}_i = \sum_{k=1}^K \hat{p}_{ik}/K$. Epistemic uncertainty corresponds to the mutual information between the parameters of the model and the true label of the sample. Low epistemic uncertainty thus means that the model parameters would not change significantly if trained on the true label, suggesting that the prediction is indeed correct. The cumulative effect of many correct pseudo-labels added over time, however, provides a strong enough training signal to push the model towards better-performing parameters, as we show in the experimental results.

3.4 Pseudo-labeling

The estimated epistemic uncertainty (Eq. 7) is used to rank and select unlabeled examples for pseudo-labeling. Let $\rho(i)$ denote the rank of sample i . Then, the set L^{new} of newly pseudo-labeled samples is formed by taking the T samples with lowest uncertainty from U , ensuring that it is lower than a threshold t_l :

$$L^{\text{new}} = \{i \in U | \rho(i) \leq T \wedge u_i^e \leq t_l\} \quad (8)$$

Previous works on semi-supervised classification have shown that balancing the pseudo-label selection between the two classes – i.e., ensuring that the ratio of newly labeled positives and negatives is close to a given target ratio r – is beneficial Rizve et al. [2021]. In this case, the set L^{new} is partitioned according to the model's predictions into a set L_+^{new} of predicted positives and L_-^{new} of predicted negatives, and the most uncertain samples in the larger set are discarded to reach the desired ratio r , which we fix to 1. We then assign soft pseudo-labels, i.e., the average prediction in the open interval $(0, 1)$, to these samples:

$$y_i = \hat{p}_i \quad \forall i \in L_-^{\text{new}} \cup L_+^{\text{new}} \quad (9)$$

As discussed previously, low epistemic uncertainty signals likely correct predictions. Using such predictions as a target in the loss \mathcal{L}_L provides a stronger, more explicit learning signal to the model, resulting in a larger decrease in risk compared to using the same example as unlabeled in

\mathcal{L}_{PU} . At the same time, soft pseudo-labels provide an additional signal regarding the estimated aleatoric uncertainty of samples. Furthermore, they help reduce overfitting and the emergence of confirmation bias in case the assigned pseudo-label is wrong by acting as dynamically-smoothed labels Müller et al. [2019], Arazo et al. [2020].

3.5 Pseudo-unlabeling

Similar to the way that low uncertainty on an unlabeled example indicates that the prediction can be trusted, high uncertainty on a pseudo-labeled example indicates that the assigned pseudo-label might not be correct after all. To avoid training on such possibly incorrect pseudo-labels, we move the pseudo-labeled examples with uncertainty above a threshold t_u back into the unlabeled set:

$$U^{\text{new}} = \{i \in L | \hat{u}_i^e \geq t_u\} \quad (10)$$

$$y_i = 0 \quad \forall i \in U^{\text{new}} \quad (11)$$

4 Experiments

To empirically compare our proposed framework to existing state-of-the-art losses and models, we followed standard protocols for PUL Kiryo et al. [2017], Kato et al. [2019], Chen et al. [2020a,b]. After presenting the main results, we empirically show the advantage of our framework in improving performance for both imbalanced and standard PU scenarios, being applicable to different data modalities, and using various losses for PU learning. Finally, we provide further analyses of PUUPL including an investigation of its sensitivity with respect to pseudo-labeling hyperparameters. The source code of the method and all the experiments are available at <https://anonymous.4open.science/r/PUUPL-BE6E>.

4.1 Experimental protocol

4.1.1 Datasets

We evaluated our method in the standard setting of MNIST Deng [2012] and CIFAR-10 Krizhevsky et al. [2009] datasets, as well as Fashion MNIST (F-MNIST) Xiao et al. [2017], CIFAR-100-20 Krizhevsky et al. [2009] and IMDB Maas et al. [2011] to show the applicability to different data modalities. Similar to previous studies Chen et al. [2020a], Kiryo et al. [2017], Kato et al. [2019], Chen et al. [2020b], positives were defined as odd digits in MNIST and vehicles in CIFAR-10. For F-MNIST we used trousers, coats, and sneakers as positives, and for the experiments on CIFAR-100-20, we defined those 10 out of the 20 superclasses as positives that correspond to living creatures (i.e., ‘aquatic mammal’, ‘fish’, ‘insects’, ‘large carnivores’, ‘large omnivores’, ‘medium-sized mammals’, ‘non-insect invertebrates’, ‘people’, ‘reptiles’, ‘small mammals’). The number of training samples is reported in Supplementary Table 6.

For all datasets, we reserved a validation set of 5,000 samples and used all other samples for training, evaluating on the canonical test set. To simulate an imbalanced setting, we downsampled the positives in the training and validation sets to obtain $\pi = 0.1$ and labeled only 600 of them. We also report results with 1,000 and 3,000 randomly chosen labeled training positives without downsampling as is common in the literature. For the image datasets, we subtracted the mean pixel intensity in the training set and divided it by the standard deviation, while for IMDB we used pre-trained GloVe embeddings of size 200 on a corpus of six billion tokens.

4.1.2 Network architectures

To ensure a fair comparison with other works in PUL Chen et al. [2020b,a], Kiryo et al. [2017], we used the same architectures on the same datasets, namely a 13-layer convolutional neural network (CNN) for the experiments on CIFAR-10 and CIFAR-100-20 (Table 7) and a multi-layer perceptron (MLP) with four fully-connected hidden layers of 300 neurons each and ReLU activation for MNIST and F-MNIST. For IMDB, we used a bidirectional LSTM network with a MLP head whose number of units was optimized as part of the hyperparameter search (Table 8).

4.1.3 Training

We trained all models with the Adam optimizer Kingma and Ba [2015] with $\beta_1 = 0.9$ and $\beta_2 = 0.999$ and an exponential learning rate decay with $\gamma = 0.99$, while learning rate, batch size, and weight decay were tuned together with the other pseudo-labeling hyperparameters using the ranges in Table 9 in the Supplements. We provide experimental results using both a PU validation set, to provide a real-world performance estimate, as well as a fully-labeled (PN) validation set to compare against state-of-the-art PUL methods that used such a labeled validation set Chen et al. [2020b], Hu et al. [2021] and to showcase the *potential* of our method. When using a PU validation set, we used the AUROC between positive and unlabeled samples as tuning criterion, as previous work Menon et al. [2015], Jain et al. [2017] has shown that higher AUROC on PU data directly translates to higher AUROC on fully labeled data.

4.1.4 Evaluation

We obtain the final results by training the model five times with random initialization and training-validation split while using the same canonical test set, reporting the highest test accuracy obtained both with a fully-labeled (PN) and a PU validation set. Statistical significance was established with an unpaired *t*-test comparing the performance of PUUPL and the best performer amongst all other methods.

We compare PUUPL against VPU Chen et al. [2020a] and Self-PU Chen et al. [2020b] using the same network architecture and data splits. We consider the former as it does not require a known prior π and can use a PU validation set, and the latter as the state-of-the-art self-training method for PUL even though it requires a positive-negative (PN) labeled validation set. We additionally compare against a naive, uncertainty-unaware, pseudo-labeling baseline “+PL” that used the sigmoid outputs directly as a ranking measure for pseudo-labeling instead of the epistemic uncertainty, while still assigning soft pseudo-labels.

4.2 Main Results

Table 1 shows the performance of PUUPL and the other baselines in an imbalanced scenario with only 600 labeled positives and a prior $\pi = 0.1$. PUUPL was the overall best performer in all comparisons except on the MNIST dataset with PU validation, where its performance was 0.31 percentage points (p.p.) lower than the imbnnpU baseline. The increase in accuracy was statistically significant with $p < 0.0015$ in each case except for CIFAR-10 with PU validation where $p = 0.055$. On CIFAR-10 with PU validation, the improvement against the second-best was not statistically significant, while in all other cases it was with $p < 0.0015$. PUUPL improved performance the most in the IMDB dataset, where accuracy was 2.2 and 3.5 p.p. higher with PN and PU validation sets, and the improvement in CIFAR-100-20 was similarly high with 2.0 and 2.8 p.p. respectively. Self-PU struggled in this setting, collapsing to negative predictions on CIFAR-100-20 and demonstrating unstable behavior on CIFAR-10, where the collapse only

Valid.	Method	Dataset				
		MNIST	F-MN	C-100-20	CIF-10	IMDb
PN	Self-PU Chen et al. [2020b]	94.44±0.12	90.99±0.47	50.00±0.0	63.97±3.97	-
	imbnnPU Su et al. [2021]	95.65±0.11	91.54±0.18	71.61±0.73	87.59±0.26	74.44±0.61
	+PL	95.19±0.20	91.26±0.22	71.80±0.93	85.82±0.50	75.94±0.61
	+PUUPL	96.09±0.10	91.93±0.12	73.79±0.33	88.93±0.31	78.16±0.78
PU	VPU Chen et al. [2020a]	80.87±3.24	89.30±0.98	70.01±0.96	86.41±0.78	-
	imbnnPU Su et al. [2021]	95.61±0.05	89.88±0.51	67.13±1.26	87.61±0.25	74.32±0.58
	+PL	94.65±0.48	89.55±0.57	68.42±1.18	84.57±1.32	75.88±0.68
	+PUUPL	95.30±0.50	91.86±0.09	72.80±0.38	87.97±0.38	77.78±0.86

Table 1: Average test accuracy and its standard error over five repetitions where model training was performed with an imbalanced dataset with $\pi = 0.1$ and 600 labeled positives. The row “+PL“ refers to an uncertainty-unaware pseudo-labeling baseline, while “+PUUPL“ refers to our uncertainty-aware solution. The validation column refers to the use of a fully-labeled (PN) or PU validation set.

Valid.	Method	Dataset				
		MNIST	F-MN	C-100-20	CIF-10	IMDb
PN	Self-PU Chen et al. [2020b]	95.64±0.13	91.55±0.18	75.41±0.44	90.56±0.09	-
	nnPU Kiryo et al. [2017]	96.36±0.06	91.70±0.12	72.46±0.83	90.49±0.13	79.62±0.67
	+PL	96.22±0.13	92.09±0.12	74.07±0.71	90.56±0.11	79.04±0.39
	+PUUPL	97.02±0.08	92.13±0.09	77.39±0.31	91.12±0.04	80.43±0.40
PU	VPU Chen et al. [2020a]	93.84±0.88	91.90±0.22	72.12±1.05	87.50±1.05	-
	nnPU Kiryo et al. [2017]	95.70±0.11	90.93±0.26	72.48±0.83	90.49±0.15	79.62±0.65
	+PL	95.91±0.23	91.36±0.13	74.30±0.68	90.23±0.07	79.04±0.39
	+PUUPL	97.12±0.07	91.26±0.26	77.49±0.33	90.74±0.15	80.26±0.51

Table 2: Average test accuracy and its standard error over five repetitions on various datasets with 3,000 labeled training positives. The row “+PL“ refers to an uncertainty-unaware pseudo-labeling baseline, while “+PUUPL“ refers to our uncertainty-aware solution. The validation column refers to the use of a fully-labeled (PN) or PU validation set.

occurred in certain training-validation splits. The naive pseudo-labeling baseline that did not use uncertainty worsened performance, compared to imbnnpU, in three datasets out of five, regardless of the method used for validation. This is, hypothetically, due to the emergence of the confirmation bias.

We performed the same comparison using 3,000 labeled training positives and the natural prior of each dataset, while using the nnPU loss as \mathcal{L}_{PU} (Table 2), as well as 1,000 labeled positives (Table 10). The results were qualitatively similar, with PUUPL providing the highest test accuracy except for Fashion-MNIST, and sometimes considerable performance increase, for example almost 5 p.p. more in the case of CIFAR-100-20 with 3,000 positives compared to the nnPU baseline. For Fashion-MNIST, there was no statistically significant difference in accuracy between PUUPL and the uncertainty-unaware pseudo-labeling baseline, while in all other cases the improvement was statistically significant ($p = 0.023$ for IMDB with PN validation, $p = 0.014$ for CIFAR-10 with PU validation, and $p < 0.001$ in all other cases).

These findings substantiate the advantages of pseudo-labeling in PUL as well as the necessity of uncertainty quantification in this procedure and in particular the benefit that this brings in more imbalanced scenarios with few labeled positives or low prior.

4.2.1 PUUPL is loss-agnostic

Our framework is uniquely positioned to take advantage of newly developed risk estimators for PU learning: as we showed above, PUUPL could make use of the imbnnpU loss Su et al. [2021] and the nnPU loss Kiryo et al. [2017] to substantially improve on the state-of-the-art in the imbalanced and the general setting. Next to imbnnpU, there exists a variety of alternative PU losses for different scenarios. The nnPUSB loss Kato et al. [2019] was developed to address the issue of labeling bias in the training positives, a more general setting compared to the i.i.d. assumption of traditional PUL methods Bekker and Davis [2020]. We tested PUUPL in such a biased setting where positives in the CIFAR-10 training and validation sets were with 50% chance an airplane, 30% chance an automobile, 15% chance a ship, and 5% chance a truck. The test distribution was instead balanced, meaning for instance that test samples were half as likely to be airplanes compared to the training set, and five times more likely to be truck images. We used the same hyperparameters as for the i.i.d. CIFAR-10 experiments except for the loss \mathcal{L}_{PU} where we used the nnPUSB loss Kato et al. [2019] to handle the positive bias. The baseline with nnPUSB loss performed better than the nnPU loss but worse than PUUPL with the nnPU loss, and the best performance was achieved with PUUPL on top of the nnPUSB loss (Table 3). The improvement provided by PUUPL was statistically significant ($p < 1.07 \times 10^{-6}$ in all cases).

These results demonstrate that PUUPL can be applied even when a sampling bias is suspected by a practitioner and no *ad hoc* risk estimator is available, as our uncertainty-aware pseudo-labeling framework with the bias-oblivious nnPU loss obtained better results compared to a bias-aware risk estimator without pseudo-labeling.

4.2.2 Uncertainty quantification improves pseudo-labels

According to the results in Table 1 and 2, naive pseudo-labeling frequently reduces performance, rather than improving it; it then follows that the performance improvement of PUUPL stems from the uncertainty ranking used to select and assign pseudo-labels (Eq. 8). We investigated this in a series of experiments with PUUPL, nnPU, and the naive pseudo-labeling baseline with 1,000 labeled positives, and we found that the improvement in expected calibration error (ECE) on the test set and negative log-likelihood (NLL) of the pseudo-labels assigned by PUUPL was at least 40% and often much larger (Table 4). As shown in Figure 2, the ECE decreased during the first few pseudo-labeling rounds, after which it stabilized while the accuracy continued improving.

	PU loss	
	nnPU [Kiryo et al., 2017]	nnPUSB [Kato et al., 2019]
Only PU loss	87.05 \pm 0.14	87.31 \pm 0.12
PU loss+PUUPL	87.70 \pm 0.14	87.91 \pm 0.14

Table 3: Test accuracy of PUUPL on the CIFAR-10 dataset with a selection bias on the positive labels when using the nnPU and nnPUSB losses. Our framework improved over the base PU loss in both cases, and, in particular, PUUPL with nnPU loss achieved better performance than the nnPUSB loss alone.

	Test Expected Calibration Error (%)		
	nnPU	+PL	+PUUPL
IMDb	25.94 \pm 0.78	25.23 \pm 0.11	6.33 \pm 0.17
CIFAR-10	10.89 \pm 0.10	9.24 \pm 0.15	5.70 \pm 0.72
CIFAR-100-20	31.62 \pm 0.29	27.51 \pm 0.59	22.12 \pm 0.39
	Pseudo-labels Negative Log-Likelihood		
	nnPU	+PL	+PUUPL
IMDb	-	2.74 \pm 0.19	0.61 \pm 0.02
CIFAR-10	-	0.66 \pm 0.05	0.29 \pm 0.03
CIFAR-100-20	-	3.76 \pm 0.29	0.94 \pm 0.05

Table 4: Expected calibration error (ECE) on the test set using 1,000 labeled positives for training (average and standard error over five runs), as well as negative log-likelihood of the assigned pseudo-labels against the true labels.

We also observed that a larger improvement in pseudo-label quality corresponds to a larger improvement in predictive performance.

4.2.3 Robustness of PUUPL

Prior misspecification An important concern for practitioners is how to determine the prior π of a PU dataset, as in the case of sub-optimal estimation the performance of the PU classifier can be harmed considerably. Prior estimation constitutes a whole research branch in PUL Chen et al. [2020a], Garg et al. [2021] and is a significant challenge in any practical PU application Bekker and Davis [2020]. Some contemporary methods for PUL Chen et al. [2020b], Acharya et al. [2022], Zhao et al. [2022], Hammoudeh and Lowd [2020] assume a known prior and do not discuss the practical consequences of not knowing such parameter, while other methods incorporate prior estimation directly into the training procedure Chen et al. [2020a], Garg et al. [2021], Hu et al. [2021]. We treated π as a hyperparameter optimized using the AUROC on a PU validation set as a criterion Menon et al. [2015], Jain et al. [2017], thus bridging the gap between estimating the prior during training and assuming it is known *a priori*.

Our experimental results show that optimizing the prior in such a way resulted in a consistent reduction in test accuracy between 0.8 and 1.2 percentage points for our framework, the PU loss, and the naive pseudo-labeling baseline (PU sections in Tables 1 and 2). In a similar vein, methods

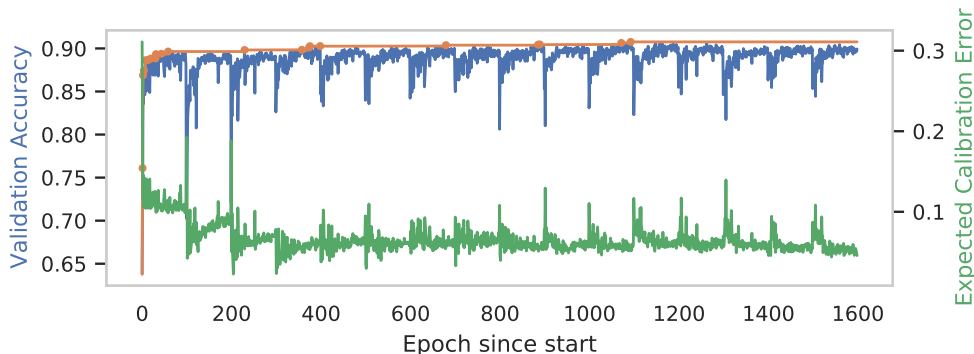


Figure 2: Validation accuracy (left, blue) and expected calibration error (ECE, right, green) for a run on CIFAR-10 with 1,000 positives. Note the substantial reduction in ECE in the second and third pseudo-labeling iterations, when the ensemble is trained on soft labels. The orange line indicates the best validation accuracy at each epoch, with the new highest accuracy marked by orange dots. The overall highest was 90.76% at epoch 1092, corresponding to a test accuracy of 90.35%.

such as VPU that optimize the prior as part of the training procedure show a similar or larger difference compared to methods that use a PN labeled validation set such as Self-PU. However, in most cases, PUUPL remained the top performer in both settings.

Moreover, training using a wrong value for π was less harmful to PUUPL compared to nnPU only (Fig. 3a). For example, on CIFAR-10 the test accuracy showed a wide plateau around the true prior of 0.4 with a performance reduction of less than 2.5% in the range $[0.3, 0.6]$. With smaller priors, the nnPU loss collapsed to constantly predicting the majority class, and specialized oversampled risk estimators Su et al. [2021] were needed to cope with such a setting (we showed the effectiveness of PUUPL in imbalanced settings in the previous section). Furthermore, the performance gap between PUUPL and nnPU widened as π was more severely misspecified, indicating a higher degree of robustness.

Number of labeled training positives The performance of PUUPL steadily increased and seemed to plateau at 91.4% at 3,000 labeled positives (Fig. 3b). The gap between nnPU and PUUPL was largest in the low labeled data region with a 1.44% gap at 250 labels, where PUUPL achieved 87.59% accuracy, shrinking to a gap of 0.52% with 3,000 labels, where PUUPL’s performance was 91.44%. This supports our intuition about the importance of accounting for prediction uncertainty because, as the amount of labeled data decreases, uncertainty becomes more important to detect overfitting and prevent the model from assigning incorrect pseudo-labels.

Loss mixing parameter As a loss, PUUPL uses a convex combination of a loss for the assigned pseudo-labels and the remaining PU data using a mixing coefficient λ (Eq. 1). The best performing combination used $\lambda = 0.1$, with modest performance reduction until $\lambda = 0.5$ (Fig. 3c), with too small values nullifying the effect of pseudo-labeling, and larger values harming performance. In general, when too few samples are pseudo-labeled, the loss \mathcal{L}_L is a high variance estimator of the classification risk, and thus should not be weighted excessively. This effect may be reduced as more pseudo-labels are added, and dynamic adaptation of λ over training could provide an additional performance improvement.

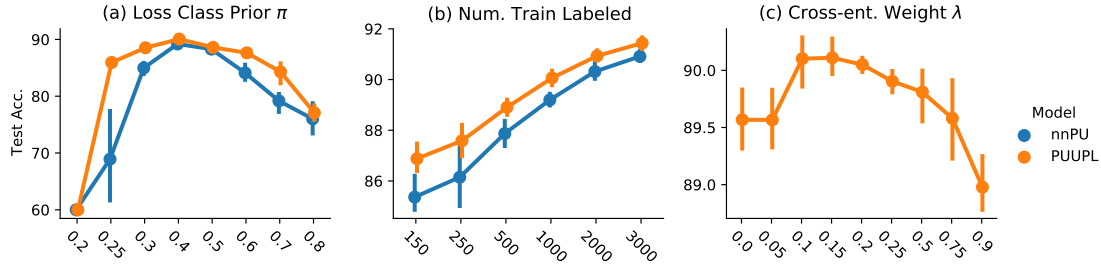


Figure 3: Mean and standard deviation of the CIFAR-10 test accuracy obtained over five runs when training with wrong prior (a), number of training labeled positives (b) and different loss combination parameter λ (c). PUUPL proved to be more robust to prior misspecification (true $\pi = 0.4$), as the performance degradation was considerably reduced over a wide range of values. It was also more robust to the lower number of labeled samples, as the gap between our framework and nnPU widened when fewer labeled positives were available for training (note the different y -axes scales).

4.3 Real-world application

In this section we show the applicability and benefits of PUUPL to a real-world imbalanced dataset with applications related to healthcare, improving the predictive performance of previous methods developed *ad hoc*. Cancer is the result of malignant mutations that were not wiped out in time by the immune system. It is however possible to instruct the immune system to fight the tumor through specific vaccines that contain neo-epitopes that arose as a result of those mutations, i.e., short genomic regions surrounding the mutated sites that can trigger an immune response [Hu et al., 2017]. Such vaccines can be designed computationally by solving an optimization problem that chooses the most promising mutations to target while ensuring that the vaccine can be processed appropriately by the body Dorigatti and Schubert [2020b,a], Toussaint et al. [2011]. One of the main steps of such processing Blum et al. [2013] is the digestion of the vaccine by the proteasome, a tubular protein complex that degrades old or misfolded proteins into shorter fragments (Fig. 4). In order for the vaccine to be effective these pieces must correspond to the neoantigens originally contained in the vaccine. Therefore, accurately predicting proteasomal cleavage, i.e., the position where a sequence is cut, is very important to design more effective vaccines. Modern high-throughput pipelines [Purcell et al., 2019] are able to detect MHC-presented epitopes on the cell surface (Fig. 4) which must have originated from proteasomal cleavage. While missed cleavage sites are never measured, not all presented epitopes are detected, and not all peptides resulting from proteasomal cleavage are presented. Thus, PUL is a natural abstraction of proteasomal cleavage prediction.

4.3.1 Dataset

We collected a dataset of 294,615 MHC-I epitopes from the IEDB Vita et al. [2018] database and 89,853 from the Human MHC Ligand Atlas Marcu et al. [2019]. To identify the potential progenitor protein of each epitope, we used BLAST [Altschul et al., 1990] and filtered for epitopes with a unique progenitor protein resulting in a total of 258,424 data points. Through the progenitor protein, we recovered the residues preceding the N-terminus and following the C-terminus of the epitope, thus providing context for the cleavage predictor. We generated two separate datasets based exclusively on N- or C-termini cleavage sites, as it is known that the biological signal differs in these two situations [Schatz et al., 2008]. We generated “decoy” samples by considering cleavage sites located within three residues of the experimentally-determined terminus; as discussed

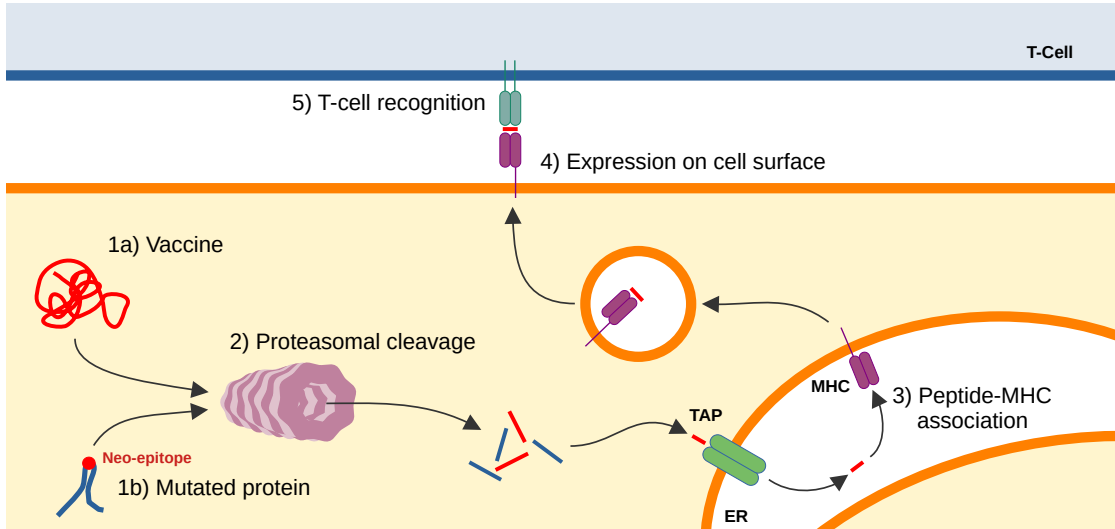


Figure 4: Predicting the outcome of each event in the antigen processing pathway [Blum et al., 2013] is crucial to enable the design of epitope vaccines. Vaccines ingested by antigen presenting cells (1a) as well as mutated proteins produced by cancerous cells (1b) are cleaved in short fragments by the proteasome (2). Some of these fragments, or peptides, are then transported into the endoplasmic reticulum (ER) through the Transporter associated with Antigen Processing (TAP). A fraction of these peptides bind to the Major Histocompatibility Complex (MHC, 3) and the resulting construct is then expressed on the cell surface (4), where they can be inspected by passerby T-cells and possibly trigger an appropriate immune response (5).

previously, it is unknown whether cleavage could or could not have happened at those positions, hence we treat such decoys as unlabeled in our PUL training procedure. The final datasets were then composed of 1,285,659 samples with 229,163 positives for the N-terminus datasets and 1,277,344 samples with 222,181 positives for the C-terminus datasets.

4.3.2 Modeling, Training, and Evaluation

Each sequence contains ten amino acids, each of which was one-hot encoded and processed by a MLP. We used imbnnPU [Su et al., 2021] as \mathcal{L}_{PUL} . For imbnnPU and PUUPL we report the cross-validation scores and use the statistical test proposed by [LeDell et al., 2015] to estimate the AUROC, its standard error, and confidence intervals. Note that, as we do not know the true negatives, traditional metrics to evaluate classification performance such as accuracy, F1, precision, recall, etc. are not applicable. As external baselines we consider NetChop [Nielsen et al., 2005] and NetCleave [Amengual-Rigo and Guallar, 2021], evaluating their predictions on ten random bootstraps of our dataset. These baselines are based on MLPs and convolutional neural networks respectively and, importantly, they approach the problem as a supervised binary classification task, treating decoy samples as negatives rather than unlabeled. We also present evaluation scores for the imbnnPU loss Su et al. [2021], commonly used for PUL on imbalanced datasets.

	AUROC	
	N-terminal	C-terminal
NetChop 20S	52.72±0.02	66.07±0.02
NetChop C term	50.99±0.02	81.53±0.01
NetCleave	49.27±0.02	79.61±0.01
imbnnPU	75.15±0.06	83.99±0.06
PUUPL	78.00±0.06	87.20±0.04

Table 5: Average and standard error of area under the ROC curve (AUROC) on both datasets for NetChop, NetCleave, the imbnnPU loss and PUUPL.

4.3.3 Results

Both PUUPL and the imbnnPU loss achieved lower performance on the N-terminals dataset, confirming previous observations that this predictive task is harder due to the biological processes involved [Schatz et al., 2008]. On the C-terminal dataset, the imbnnPU loss improved performance by 2.5 and 4.4 points compared to NetChop and NetCleave respectively, and PUUPL added a further 3.2 points reaching 87.2% AUROC (Table 5). In both datasets the difference in AUROC between imbnnPU and PUUPL was statistically significant at a significance of 1%: the confidence intervals are [74.99, 75.32] and [77.85, 78.15] for N-terminals, and [83.85, 84.14] and [87.08, 87.32] for C-terminals. Note that both NetChop and NetCleave were only trained on C-terminals cleavage sites in the original publication, thus explaining their random predictions on the N-terminals dataset.

5 Discussion and conclusions

We introduced PUUPL, an uncertainty-aware pseudo-labeling framework for PUL that uses the epistemic uncertainty of an ensemble of networks to select which examples to pseudo-label. We conducted extensive experiments to demonstrate the benefits of our approach and show its reliability in settings that are likely to be encountered in the real world such as heavily imbalanced settings with small π and few labeled positives, a bias in the positive training data, the unavailability of labeled negatives for validation, and the misspecification of the class prior π . Unlike many alternative methods, PUUPL can be applied to learning problems in any domain out of the box as it does not rely on regularization methods that are restricted to a specific data modality, most frequently images, such as mixup Zhang et al. [2018] (used by Chen et al. [2020a], Zhao et al. [2022]) or contrastive representations (used by Acharya et al. [2022]). Furthermore, it is easy to adapt as it builds on standard methods (unlike Chen et al. [2020b]), and does not require pretrained representations to work (as Hammoudeh and Lowd [2020] does). We further used our framework to advance the state-of-the-art on a real-world healthcare dataset with potential repercussions on efficacy and deployment cost of personalized epitope vaccines for cancer treatment.

Our choice of deep ensembles was rooted in their competitiveness in empirical benchmarks Ovardia et al. [2019]. However, PUUPL can easily be extended to take advantage of more accurate uncertainty quantification methods as they become available Abdar et al. [2021], especially considering the computational overhead of training deep ensembles. In fact, as the matter of uncertainty quantification in deep learning is far from settled, the performance and efficiency of our

framework could be further improved by employing more accurate uncertainty quantification methods Abdar et al. [2021]. We demonstrated robustness against biased positive labels and imbalanced datasets, however, it is the practitioners' responsibility to ensure that the obtained predictions are "fair", with "fairness" defined appropriately with respect to the target application, and do not systematically affect particular subsets of the population of interest. Ultimately, we can only leave it to practitioners to use their moral and ethical judgment as to whether all stakeholders and their interests are fairly represented in their application.

To conclude, our PUUPL framework is applicable to and reaches competitive performance in heavily imbalanced settings with few positives as well as in traditional balanced datasets, even when the true prior is unknown, and can work with several data modalities including images, natural language, and proteomic data while being robust to hyperparameter selection.

Declarations

Acknowledgments We are grateful to David Rügamer, Niki Kilbertus, Bastian Rieck and the anonymous reviewers for their comments and suggestions.

Funding: Emilio Dorigatti was supported by the Helmholtz Association under the joint research school "Munich School for Data Science - MUDS" (Award Number HIDSS-0006). Jann Goschenhofer was supported by the Bavarian Ministry of Economic Affairs, Regional Development, and Energy through the Center for Analytics – Data – Applications (ADA-Center) within the framework of BAYERN DIGITAL II (20-3410-2-9-8). B. S. acknowledges financial support by the Postdoctoral Fellowship Program of the Helmholtz Zentrum München. Mina Rezaei and Bernd Bischl were supported by the German Federal Ministry of Education and Research (BMBF) under Grant No. 01IS18036A, Munich Center for Machine Learning (MCML).

Conflicts of interest/Competing interests: The authors of the manuscript do not have a conflict of interest.

Authors' contributions: The method was conceived by E.D. and finalized upon discussion with all other authors. All authors contributed to the experimental protocol, while the implementation was performed by E.D. and J.G., who also performed the experiments. All authors contributed to the interpretation of the results. The manuscript was written by E.D. and J.G. with feedback from all other authors. All authors read and approved the final manuscript.

Dataset	Train Pos.	Train Neg.	Test Size
MNIST	30,508	29,492	10,000
F-MNIST	30,000	30,000	10,000
CIFAR-10	20,000	30,000	10,000
CIFAR-100-20	25,000	25,000	10,000
IMDb	12,500	12,500	25,000

Table 6: Size of test set and number of positives and negatives in the training set for each dataset.

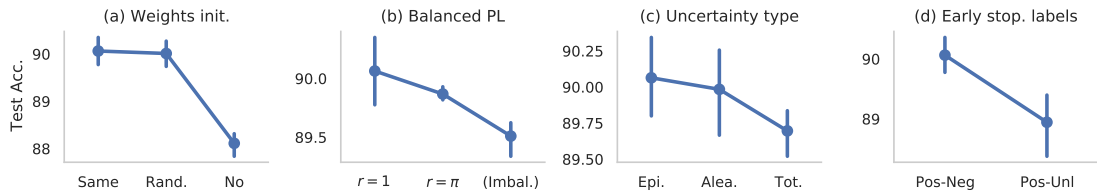


Figure 5: Mean and standard deviation of the test accuracy obtained over five runs by different variations of our *PUUPL* algorithm: (a) different weight initialization at each iteration, (b) balanced or imbalanced PL selection, (c) type of uncertainty, (d) whether to use PN or PU validation set. Note the different scales on the y -axes.

Appendix A Network architecture, hyperparameters and datasets

Table 6 reports the number of samples in each dataset. Table 7 reports the network architecture used in the CIFAR-10 and CIFAR-100-20 experiments, while Table 8 reports the network used with IMDb. Table 9 reports the hyperparameters related to pseudo-labeling and their ranges.

Appendix B Further results and sensitivity analyses

Table 10 reports the test accuracy when 1,000 labeled positives were used for training.

We performed ablation studies on the CIFAR-10 dataset by changing one parameter at a time of the best configuration found by Hyperband, training and evaluating with five different splits, and reporting the test accuracy corresponding to the best validation score for each run. To limit the computational resources needed, we used at most 15 pseudo-labeling iterations.

Weight initialization: We confirmed the observation that it is beneficial to re-initialize the weights after each pseudo-labeling step Arazo et al. [2020], with slightly better performance (+0.052%) achieved when the weights are re-initialized to the same values before every pseudo-labeling iteration (Fig. 5a). We believe this encourages the model to be consistent across pseudo-labeling rounds.

Uncertainty: Ranking predictions by aleatoric performance was almost as good as ranking by epistemic uncertainty (-0.08%), while total uncertainty produced moderately worse rankings (-0.37% , Fig. 5c). An ensemble with only two networks achieved the best performance, while larger ensembles performed worse, and Monte Carlo dropout (-0.85%) was better than ensembles of five (-1.00%) and ten networks (-1.58%).

Layer type	Layer parameters
Conv. 2D	InC=3, OutC=96, k=3, s=1, p=1
Dropout	p=0.15
Batch Norm.	eps=1e-05, momentum=0.1
ReLU	
Conv. 2D	InC=96, OutC=96, k=3, s=1, p=1
Dropout	p=0.15
Batch Norm.	eps=1e-05, momentum=0.1
ReLU	
Conv. 2D	InC=96, OutC=96, k=3, s=2, p=1
Dropout	p=0.15
Batch Norm.	eps=1e-05, momentum=0.1
ReLU	
Conv. 2D	InC=96, OutC=192, k=3, s=1, p=1
Dropout	p=0.15
Batch Norm.	eps=1e-05, momentum=0.1
ReLU	
Conv. 2D	InC=192, OutC=192, k=3, s=1, p=1
Dropout	p=0.15
Batch Norm.	eps=1e-05, momentum=0.1
ReLU	
Conv. 2D	InC=192, OutC=192, k=3, s=2, p=1
Dropout	p=0.15
Batch Norm.	eps=1e-05, momentum=0.1
ReLU	
Conv. 2D	InC=192, OutC=192, k=3, s=1, p=1
Dropout	p=0.15
Batch Norm.	eps=1e-05, momentum=0.1
ReLU	
Conv. 2D	InC=192, OutC=192, k=1, s=1, p=0
Dropout	p=0.15
Batch Norm.	eps=1e-05, momentum=0.1
ReLU	
Conv. 2D	InC=192, OutC=10, k=1, s=1, p=0
Dropout	p=0.15
Batch Norm.	eps=1e-05, momentum=0.1
ReLU	
Flatten	
Linear	in features=640, out features=1000, bias=yes
ReLU	
Linear	in features=1000, out features=1000, bias=yes
ReLU	
Linear	in features=1000, out features=1, bias=yes

Table 7: Network architecture used for the CIFAR-10 experiments. InC: input channels, OutC: output channels, k: kernel size, s: stride, p: padding

Layer type	Layer parameters
LSTM	input size=200, hidden size=128, num layers=2, dropout=0.25, bidirectional=True
Dropout	p=0.2
Linear	in features=256, out features=196, bias=True
Batch Norm.	eps=1e-05, momentum=0.1
ReLU	
Dropout	p=0.2
Linear	in features=196, out features=196, bias=True
Batch Norm.	eps=1e-05, momentum=0.1
ReLU	
Linear	in features=196, out features=1, bias=True

Table 8: Network architecture used for the IMDb experiments

Hyper-parameter	Value range
Estimator	Ensemble or MC Dropout
Number of samples	[2, 25]
Uncertainty type	Aleatoric, epistemic, total
Max. new labels T	[100, 5000]
Max. new label uncertainty t_l	[0, $-\log 2$]
Min. unlabeled uncertainty t_u	[0, $-\log 2$]
Reassign all pseudo-labels	Yes or no
Re-initialize to same weights	Yes or no
Cross-entropy weight λ	[0, 1]

Table 9: Pseudo-labeling hyperparameters

Valid.	Method	Dataset				
		MNIST	F-MN	C-100-20	CIF-10	IMDb
PN	Self-PU Chen et al. [2020b]	93.09±0.16	90.21±0.15	70.56±0.62	88.33±0.18	-
	nnPU Kiryo et al. [2017]	94.68±0.13	90.55±0.08	67.69±0.23	88.87±0.17	71.45±0.38
	+PL	95.32±0.24	90.69±0.09	69.01±0.56	90.02 ±0.09	71.70±0.14
	+PUUPL	96.09 ±0.08	90.92 ±0.07	71.44 ±0.37	89.84±0.13	74.14 ±0.35
PU	VPU Chen et al. [2020a]	89.78±0.76	85.50±0.63	69.58±1.47	85.06±0.55	-
	nnPU Kiryo et al. [2017]	93.89±0.38	89.53±0.61	67.25±0.98	87.73±0.32	71.43±0.39
	+PL	92.16±0.50	90.63 ±0.33	67.93±0.49	88.92 ±0.19	71.44±0.28
	+PUUPL	94.85 ±0.08	90.05±0.17	69.92 ±0.70	88.82±0.16	73.98 ±0.25

Table 10: Average test accuracy and its standard error over five repetitions on various datasets with 1,000 labeled training positives. The row “+PL“ refers to an uncertainty-unaware pseudo-labeling baseline, while “+PUUPL“ refers to our uncertainty-aware solution. The validation column refers to the use of a fully-labeled (PN) or PU validation set.

Early stopping: Finally, performing early stopping on the validation PU loss resulted in worse accuracy (−1.12%) compared to using the accuracy on PN labels (Fig. 5d). Although considerable when compared to the impact of other algorithmic choices, such a performance drop indicates that *PUUPL* can be used effectively in real-world scenarios when no labeled validation data are available.

Pseudo-labeling hyperparameters: Our method was fairly robust to the maximum number T of assigned pseudo-labels and the maximum uncertainty threshold t_l for the pseudo-labels, with almost constant performance up to $T = 1000$ and $t_l = 0.1$. The best performance was achieved by the combination having $T = 1000$ and $t_l = 0.05$, but both of these experiments were performed while disabling the other constraint (i.e., setting $T = \text{inf}$ when testing t_l and vice-versa). Using only a constraint on T resulted in a reduction of −0.11%, while constraining t_l alone resulted in a reduction of −1.04%. The results for t_u were less conclusive than for the general trend, possibly because values lower than 0.35 require more than the 15 pseudo-labeling iterations we used for the experiment, and values above 0.4 did not show significant differences.

Moreover, soft pseudo-labels were preferred over hard ones (+0.75%). Contrary to expectation, however, re-assigning all pseudo-labels at every iteration slightly harmed performance (−0.12%); instead, pseudo-labels should be kept fixed after being assigned for the first time. A possible explanation is that fixed pseudo-labels prevent the model’s predictions from drifting too far away from the initial pseudo-labeling towards an incorrect assignment, and thus contribute in mitigating the sort of confirmation bias that frequently plagues pseudo-labeling-based methods. It was also beneficial to assign the same number of positive and negative pseudo-labels compared to keeping the same ratio π of positives and negatives found in the whole dataset (−0.20%) or not balancing the selection at all (−0.55%). This prevents the pseudo-labeled set from becoming too imbalanced over time, a natural tendency deriving from the inherent imbalance between positive and unlabeled samples in the training set.

Appendix C Ethics statement and broader impact

Improving performance of PUL methods will catalyze research in areas where PU datasets are endemic and manual annotation is expensive or negative samples are impossible to obtain – for

example, in bioinformatics and medical applications – which ultimately benefits human welfare and well-being. The explicit incorporation of uncertainty quantification further increases the trustworthiness and reliability of PUUPL’s predictions. However, such advances in PUL could also reduce the resources required to create unwanted mass-surveillance systems by governments and/or private companies.

References

- Moloud Abdar, Farhad Pourpanah, Sadiq Hussain, Dana Rezazadegan, Li Liu, Mohammad Ghavamzadeh, Paul Fieguth, Xiaochun Cao, Abbas Khosravi, U Rajendra Acharya, et al. A review of uncertainty quantification in deep learning: Techniques, applications and challenges. *Information Fusion*, 76:243–297, 2021.
- Anish Acharya, Sujay Sanghavi, Li Jing, Bhargav Bhushanam, Dhruv Choudhary, Michael G. Rabbat, and Inderjit S. Dhillon. Positive unlabeled contrastive learning. *ArXiv*, abs/2206.01206, 2022.
- Stephen F. Altschul, Warren Gish, Webb Miller, Eugene W. Myers, and David J. Lipman. Basic local alignment search tool. *Journal of Molecular Biology*, 215(3):403–410, October 1990. doi: 10.1016/s0022-2836(05)80360-2.
- Pep Amengual-Rigo and Victor Guallar. NetCleave: an open-source algorithm for predicting c-terminal antigen processing for MHC-i and MHC-II. *Scientific Reports*, 11(1), June 2021. doi: 10.1038/s41598-021-92632-y.
- Eric Arazo, Diego Ortego, P. Albert, N. O’Connor, and Kevin McGuinness. Pseudo-labeling and confirmation bias in deep semi-supervised learning. *2020 International Joint Conference on Neural Networks (IJCNN)*, pages 1–8, 2020.
- Harotune K Armenian and Abraham M Lilienfeld. The distribution of incubation periods of neoplastic diseases. *American journal of epidemiology*, 99(2):92–100, 1974.
- Jessa Bekker and Jesse Davis. Learning from positive and unlabeled data: A survey. *Machine Learning*, 109(4):719–760, 2020.
- William H Beluch, Tim Genewein, Andreas Nürnberger, and Jan M Köhler. The power of ensembles for active learning in image classification. In *Proceedings of the IEEE/CVF Conference on Computer Vision and Pattern Recognition*, pages 9368–9377, 2018.
- Janice S. Blum, Pamela A. Wearsch, and Peter Cresswell. Pathways of antigen processing. *Annual Review of Immunology*, 31(1):443–473, March 2013. doi: 10.1146/annurev-immunol-032712-095910.
- Olivier Chapelle, Bernhard Scholkopf, and Alexander Zien. Semi-supervised learning. *Cambridge, Massachusetts: The MIT Press View Article*, 2009.
- Hui Chen, Fangqing Liu, Yin Wang, Liyue Zhao, and Hao Wu. A variational approach for learning from positive and unlabeled data. In *Advances in Neural Information Processing Systems*, pages 14844–14854, 2020a.
- Xuxi Chen, Wuyang Chen, Tianlong Chen, Ye Yuan, Chen Gong, Kewei Chen, and Zhangyang Wang. Self-pu: Self boosted and calibrated positive-unlabeled training. In *International Conference on Machine Learning*, pages 1510–1519. PMLR, 2020b.
- Marthinus Christoffel, Gang Niu, and Masashi Sugiyama. Class-prior estimation for learning from positive and unlabeled data. In *Asian Conference on Machine Learning*, volume 45 of *Proceedings of Machine Learning Research*, pages 221–236, 2016.

- Li Deng. The mnist database of handwritten digit images for machine learning research. *IEEE Signal Processing Magazine*, 29(6):141–142, 2012.
- Emilio Dorigatti and Benjamin Schubert. Graph-theoretical formulation of the generalized epitope-based vaccine design problem. *PLOS Computational Biology*, 16(10):e1008237, October 2020a. doi: 10.1371/journal.pcbi.1008237.
- Emilio Dorigatti and Benjamin Schubert. Joint epitope selection and spacer design for string-of-beads vaccines. *Bioinformatics*, 36(Supplement_2):i643–i650, December 2020b. doi: 10.1093/bioinformatics/btaa790.
- Marthinus C Du Plessis, Gang Niu, and Masashi Sugiyama. Analysis of learning from positive and unlabeled data. *Advances in neural information processing systems*, 27:703–711, 2014.
- Saurabh Garg, Yifan Wu, Alexander J Smola, Sivaraman Balakrishnan, and Zachary Lipton. Mixture proportion estimation and pu learning: a modern approach. In M. Ranzato, A. Beygelzimer, Y. Dauphin, P.S. Liang, and J. Wortman Vaughan, editors, *Advances in Neural Information Processing Systems*, volume 34, pages 8532–8544, 2021.
- Jakob Gawlikowski, Cedric Rovile Njietcheu Tassi, Mohsin Ali, Jongseo Lee, Matthias Humt, Jianxiang Feng, Anna Kruspe, R. Triebel, P. Jung, R. Roscher, M. Shahzad, Wen Yang, R. Bamler, and Xiaoxiang Zhu. A survey of uncertainty in deep neural networks. *ArXiv*, abs/2107.03342, 2021.
- Vladimir Gligorijević, P Douglas Renfrew, Tomasz Kosciolk, Julia Koehler Leman, Daniel Berenberg, Tommi Vatanen, Chris Chandler, Bryn C Taylor, Ian M Fisk, Hera Vlamakis, et al. Structure-based protein function prediction using graph convolutional networks. *Nature communications*, 12(1):1–14, 2021.
- Zayd Hammoudeh and Daniel Lowd. Learning from positive and unlabeled data with arbitrary positive shift. In H. Larochelle, M. Ranzato, R. Hadsell, M.F. Balcan, and H. Lin, editors, *Advances in Neural Information Processing Systems*, volume 33, pages 13088–13099, 2020.
- Yu-Guan Hsieh, Gang Niu, and Masashi Sugiyama. Classification from positive, unlabeled and biased negative data. In Kamalika Chaudhuri and Ruslan Salakhutdinov, editors, *Proceedings of the 36th International Conference on Machine Learning*, volume 97 of *Proceedings of Machine Learning Research*, pages 2820–2829, 09–15 Jun 2019.
- Wenpeng Hu, Ran Le, Bing Liu, Feng Ji, Jinwen Ma, Dongyan Zhao, and Rui Yan. Predictive adversarial learning from positive and unlabeled data. *Proceedings of the AAAI Conference on Artificial Intelligence*, 35(9):7806–7814, May 2021.
- Zhuting Hu, Patrick A. Ott, and Catherine J. Wu. Towards personalized, tumour-specific, therapeutic vaccines for cancer. *Nature Reviews Immunology*, 18(3):168–182, 2017. ISSN 1474-1733, 1474-1741. doi: 10.1038/nri.2017.131.
- Eyke Hüllermeier and Willem Waegeman. Aleatoric and epistemic uncertainty in machine learning: An introduction to concepts and methods. *Machine Learning*, 110(3):457–506, 2021.
- Ahmet Iscen, Giorgos Tolias, Yannis Avrithis, and Ondrej Chum. Label propagation for deep semi-supervised learning. In *Proceedings of the IEEE/CVF Conference on Computer Vision and Pattern Recognition*, pages 5070–5079, 2019.
- Shantanu Jain, Martha White, and Predrag Radivojac. Recovering true classifier performance in positive-unlabeled learning. *Proceedings of the AAAI Conference on Artificial Intelligence*, 31(1), Feb. 2017.
- Hiroataka Kaji, Hayato Yamaguchi, and Masashi Sugiyama. Multi task learning with positive and unlabeled data and its application to mental state prediction. In *2018 IEEE International Conference on Acoustics, Speech and Signal Processing (ICASSP)*, pages 2301–2305, 2018. doi: 10.1109/ICASSP.2018.8462108.

- Masahiro Kato, Takeshi Teshima, and Junya Honda. Learning from positive and unlabeled data with a selection bias. In *International Conference on Learning Representations*, 2019.
- Diederik P. Kingma and Jimmy Ba. Adam: A method for stochastic optimization. *CoRR*, abs/1412.6980, 2015.
- Ryuichi Kiryo, Gang Niu, Marthinus C du Plessis, and Masashi Sugiyama. Positive-unlabeled learning with non-negative risk estimator. *Advances in Neural Information Processing Systems*, 2017.
- Alex Krizhevsky, Geoffrey Hinton, et al. Learning multiple layers of features from tiny images. *Citeseer*, 2009.
- Balaji Lakshminarayanan, Alexander Pritzel, and Charles Blundell. Simple and scalable predictive uncertainty estimation using deep ensembles. In I. Guyon, U. V. Luxburg, S. Bengio, H. Wallach, R. Fergus, S. Vishwanathan, and R. Garnett, editors, *Advances in Neural Information Processing Systems*, volume 30, 2017.
- Erin LeDell, Maya L. Petersen, and Mark J. van der Laan. Computationally efficient confidence intervals for cross-validated area under the roc curve estimates. *Electronic journal of statistics*, 9 1:1583–1607, 2015.
- Dong-Hyun Lee. Pseudo-label: The simple and efficient semi-supervised learning method for deep neural networks. In *Workshop on Challenges in Representation Learning, ICML*, volume 3, page 896, 2013.
- Wenkai Li, Qinghua Guo, and Charles Elkan. A positive and unlabeled learning algorithm for one-class classification of remote-sensing data. *IEEE Transactions on geoscience and remote sensing*, 49(2): 717–725, 2010.
- Bing Liu, Yang Dai, Xiaoli Li, Wee Sun Lee, and Philip S Yu. Building text classifiers using positive and unlabeled examples. In *Third IEEE International Conference on Data Mining*, pages 179–186. IEEE, 2003.
- Chuan Luo, Pu Zhao, Chen Chen, Bo Qiao, Chao Du, Hongyu Zhang, Wei Wu, Shaowei Cai, Bing He, Saravanakumar Rajmohan, et al. Pulns: Positive-unlabeled learning with effective negative sample selector. In *Proceedings of the AAAI Conference on Artificial Intelligence*, volume 35, pages 8784–8792, 2021.
- Andrew L. Maas, Raymond E. Daly, Peter T. Pham, Dan Huang, Andrew Y. Ng, and Christopher Potts. Learning word vectors for sentiment analysis. In *Proceedings of the 49th Annual Meeting of the Association for Computational Linguistics: Human Language Technologies*, pages 142–150, Portland, Oregon, USA, June 2011. Association for Computational Linguistics.
- Ana Marcu, Leon Bichmann, Leon Kuchenbecker, Daniel Johannes Kowalewski, Lena Katharina Freudenmann, Linus Backert, Lena Mühlenbruch, András Szolek, Maren Lübke, Philipp Wagner, Tobias Engler, Sabine Matovina, Jian Wang, Mathias Hauri-Hohl, Roland Martin, Konstantina Kopolou, Juliane Sarah Walz, Julia Velz, Holger Moch, Luca Regli, Manuela Silgner, Michael Weller, Markus W. Löffler, Florian Erhard, Andreas Schlosser, Oliver Kohlbacher, Stefan Stevanović, Hans-Georg Rammensee, and Marian Christoph Neidert. The HLA ligand atlas - a resource of natural HLA ligands presented on benign tissues. September 2019. doi: 10.1101/778944.
- Aditya Menon, Brendan Van Rooyen, Cheng Soon Ong, and Bob Williamson. Learning from corrupted binary labels via class-probability estimation. In Francis Bach and David Blei, editors, *Proceedings of the 32nd International Conference on Machine Learning*, volume 37 of *Proceedings of Machine Learning Research*, pages 125–134, Lille, France, 07–09 Jul 2015. PMLR.
- Rafael Müller, Simon Kornblith, and Geoffrey E Hinton. When does label smoothing help? In H. Wallach, H. Larochelle, A. Beygelzimer, F. d'Alché-Buc, E. Fox, and R. Garnett, editors, *Advances in Neural Information Processing Systems*, volume 32, 2019.

- Morten Nielsen, Claus Lundegaard, Ole Lund, and Can Keşmir. The role of the proteasome in generating cytotoxic t-cell epitopes: insights obtained from improved predictions of proteasomal cleavage. *Immunogenetics*, 57(1-2):33–41, mar 2005. doi: 10.1007/s00251-005-0781-7. URL <https://doi.org/10.1007/s00251-005-0781-7>.
- Yaniv Ovadia, Emily Fertig, Jie Ren, Zachary Nado, David Sculley, Sebastian Nowozin, Joshua Dillon, Balaji Lakshminarayanan, and Jasper Snoek. Can you trust your model’s uncertainty? evaluating predictive uncertainty under dataset shift. *Advances in neural information processing systems*, 32, 2019.
- Anthony W. Purcell, Sri H. Ramarathinam, and Nicola Ternette. Mass spectrometry–based identification of MHC-bound peptides for immunopeptidomics. *Nat Protoc*, 14(6):1687–1707, may 2019. doi: 10.1038/s41596-019-0133-y.
- M. N. Rizve, Kevin Duarte, Y. Rawat, and M. Shah. In defense of pseudo-labeling: An uncertainty-aware pseudo-label selection framework for semi-supervised learning. *International Conference on Learning Representations*, 2021.
- Lukas Ruff, Robert Vandermeulen, Nico Goernitz, Lucas Deecke, Shoaib Ahmed Siddiqui, Alexander Binder, Emmanuel Müller, and Marius Kloft. Deep one-class classification. In *International conference on machine learning*, pages 4393–4402. PMLR, 2018.
- Mark M. Schatz, Björn Peters, Nadja Akkad, Nina Ullrich, Alejandra Nacarino Martinez, Oliver Carroll, Sascha Bulik, Hans-Georg Rammensee, Peter van Endert, Hermann-Georg Holzhütter, Stefan Tenzer, and Hansjörg Schild. Characterizing the n-terminal processing motif of MHC class i ligands. *The Journal of Immunology*, 180(5):3210–3217, February 2008. doi: 10.4049/jimmunol.180.5.3210. URL <https://doi.org/10.4049/jimmunol.180.5.3210>.
- Weiwei Shi, Yihong Gong, Chris Ding, Zhiheng MaXiaoYu Tao, and Nanning Zheng. Transductive semi-supervised deep learning using min-max features. In *Proceedings of the European Conference on Computer Vision (ECCV)*, pages 299–315, 2018.
- Guangxin Su, Weitong Chen, and Miao Xu. Positive-unlabeled learning from imbalanced data. In *Proceedings of the Thirtieth International Joint Conference on Artificial Intelligence*. International Joint Conferences on Artificial Intelligence Organization, aug 2021. doi: 10.24963/ijcai.2021/412.
- Daiki Tanaka, Daiki Ikami, Toshihiko Yamasaki, and Kiyoharu Aizawa. Joint optimization framework for learning with noisy labels. In *Proceedings of the IEEE Conference on Computer Vision and Pattern Recognition*, pages 5552–5560, 2018.
- Nora C. Toussaint, Yaakov Maman, Oliver Kohlbacher, and Yoram Louzoun. Universal peptide vaccines – Optimal peptide vaccine design based on viral sequence conservation. *Vaccine*, 29(47):8745–8753, November 2011. ISSN 0264410X. doi: 10.1016/j.vaccine.2011.07.132.
- Jesper E Van Engelen and Holger H Hoos. A survey on semi-supervised learning. *Machine Learning*, 109(2):373–440, 2020.
- Randi Vita, Swapnil Mahajan, James A Overton, Sandeep Kumar Dhanda, Sheridan Martini, Jason R Cantrell, Daniel K Wheeler, Alessandro Sette, and Bjoern Peters. The Immune Epitope Database (IEDB): 2018 update. *Nucleic Acids Research*, 47(D1):D339–D343, 10 2018. ISSN 0305-1048. doi: 10.1093/nar/gky1006.
- Han Xiao, Kashif Rasul, and Roland Vollgraf. Fashion-mnist: a novel image dataset for benchmarking machine learning algorithms. *arXiv preprint arXiv:1708.07747*, 2017.
- Yixing Xu, Chang Xu, Chao Xu, and Dacheng Tao. Multi-positive and unlabeled learning. In *Proceedings of the Twenty-Sixth International Joint Conference on Artificial Intelligence*, pages 3182–3188, 2017.

Hongyi Zhang, Moustapha Cisse, Yann N. Dauphin, and David Lopez-Paz. Mixup: Beyond empirical risk minimization. *International Conference on Learning Representations*, 2018.

Yunrui Zhao, Qianqian Xu, Yangbangyan Jiang, Peisong Wen, and Qingming Huang. Dist-pu: Positive-unlabeled learning from a label distribution perspective. In *Proceedings of the IEEE/CVF Conference on Computer Vision and Pattern Recognition (CVPR)*, pages 14461–14470, June 2022.